Limits of linear plasma wakefield theory for electron or positron beams

W. Lu, C. Huang, and M. M. Zhou
Department of Electrical Engineering, University of California, Los Angeles, Los Angeles, California 90095

W. B. Mori
Department of Electrical Engineering, University of California, Los Angeles, Los Angeles, California 90095 and Department of Physics and Astronomy, University of California, Los Angeles, Los Angeles, California 90095

T. Katsouleas
Department of Electrical Engineering, University of South California, Los Angeles, California 90089

(Received 2 November 2004; accepted 16 March 2005; published online 26 May 2005)

The validity and usefulness of linear wakefield theory for electron and positron bunches is investigated. Starting from the well-known Green's function for a cold-fluid plasma, engineering formulas for the maximum accelerating field for azimuthally symmetric bi-Gaussian beams of the form $n_b = n_b e^{-r^2/2\sigma_r^2} e^{-z^2/2\sigma_z^2}$ are derived. It is also found that for fixed beam parameters the optimum wake is obtained for $k_p\sigma_z = 2^{1/2}$, for $k_p\sigma_r \leqslant 1$. The validity and usefulness of linear-fluid theory is studied using fully nonlinear particle-in-cell simulations. It is found that linear theory can be useful beyond the nominal range of validity for narrow bunches. The limits of usefulness differ significantly between electron and positron bunches. For electron bunches, scaling laws are found for three limits for optimal plasma density ($k_p\sigma_z = 2^{1/2}$), characterized by the normalized spot size $k_p\sigma_r$ and the normalized charge per unit length of the beam, $\Lambda \equiv (n_b/n_p)k_p^2\sigma_r^2$. These are $\varepsilon \equiv eE/mc\omega_p = 1.3(n_b/n_p)$ for $k_p\sigma_r > 1$ and $n_b/n_p < 1$, $\varepsilon = 1.3\,\Lambda\,\ln(1/k_p\sigma_r)$, for $(\Lambda/10)^{1/2} < k_p\sigma_r < 1$ and $\Lambda < 1$, and $\varepsilon = 1.3\,\Lambda\,\ln([10/\Lambda]^{1/2})$, for $k_p\sigma_r < (\Lambda/10)^{1/2}$ and $\Lambda < 1$. Linear theory breaks down for $n_b/n_p \cong 10$. On the other hand, for positron drivers linear-fluid theory breaks down for $n_b/n_p \geqslant 1$ independent of spot size. © *2005 American Institute of Physics.*
[DOI: 10.1063/1.1905587]

I. INTRODUCTION

Recently there has been much interest in plasma wakefields for narrow charged particle bunches.[1–6] Although the Green's function for three-dimensional (3D) linear plasma wakefields is well known,[7,8] recent works have applied this in various limits to obtain approximate expressions. While there is no confusion in the literature over the 1D or wide beam limit in which the beam size is large compared to the plasma skin depth c/ω_p, there are several formulas in the literature for the narrow beam limit.[3,4] Here we attempt to provide a clear and systematic derivation for the linear wakefields in the narrow beam limit. Expressions for the wakes generated by beams with a Gaussian longitudinal profile and either a Gaussian or flat top transverse profile will be derived. For very narrow beams, the linear theory expression for the wake amplitude diverges logarithmically with the inverse of the spot size. It is shown that this unphysical divergence saturates when the normalized peak beam density n_{b0}/n_p exceeds $\sim$10 for electron drivers and $\sim$1 for positron drivers. We show that the previously obtained scaling law in which the wake amplitude increases with the inverse square of the bunch length must be modified by a weak logarithmic function of the beam spot size σ_r. We will show through fully nonlinear particle-in-cell (PIC) simulations that the linear theory expressions can still be accurate even when the fluid model breaks down in principle.

II. LINEAR THEORY

The starting point for our work is the well-known Green's function solution for the plasma response to an arbitrary relativistic charge bunch of the form $\rho_b = \rho_\perp(r)\rho_\parallel(\xi)$,[8] where $\xi = z - ct$,

$$E_z(r,\xi) = Z'(\xi)R(r) \tag{1}$$

and

$$Z'(\xi) = -4\pi\int_\xi^\infty d\xi'\,\rho_\parallel(\xi')\cos k_p(\xi-\xi'), \tag{2}$$

$$R(r) = \frac{k_p^2}{2\pi}\int_0^{2\pi} d\theta\int_0^\infty r'dr'\,\rho_\perp(r')K_0(k_p|\vec{r}-\vec{r}\,'|), \tag{3}$$

where K_0 is the zero-order modified Bessel function.

Next, we evaluate these expressions for a Gaussian longitudinal profile $\rho_\parallel(\xi) = qn_b e^{-\xi^2/2\sigma_z^2}$ at a position along the axis where $\xi \ll -\sigma_z$. Here q is the particle charge ($+e$ for a positron or proton beam and $-e$ for electron beam). The result is

$$E_z(0,\xi) = \{\sqrt{2\pi}(q/e)(mc\omega_p/e)(n_b/n_p) \times (k_p\sigma_z e^{-k_p^2\sigma_z^2/2})R(0)\}\cos(k_p\xi), \tag{4}$$

where

$$R(0) = k_p^2\int_0^\infty r'dr'\,\rho_\perp(r')K_0(k_pr'). \tag{5}$$

For wide beams, i.e., where $\rho_\perp = 1$ for $r' = 0$ and remains close to unity for r' much larger than k_p^{-1}, $R(0) \approx 1$. In this limit, it is straightforward to show that for fixed bunch length σ_z, and normalized beam density, n_b/n_p, the expression for E_z is maximized at $\varepsilon \equiv eE/mc\omega_p = [2(\pi)^{1/2}/e]\ n_b/n_p \cong 1.3 n_b/n_p$ for $k_p\sigma_z = \sqrt{2}$, which is the well-known 1D result.

The expression for $R(0)$ for a flat top beam of radius a with $\rho_\perp(r) = 1$ for $0 < r < a$ and 0 for $r > a$ is

$$R(0) = k_p^2 \int_0^a r' dr' K_0(k_p r') = 1 - k_p a K_1(k_p a), \tag{6}$$

which was given and was plotted numerically in Ref. 8. For $k_p a \ll 1$, Eq. (6) can be expanded asymptotically as

$$R(0) = \frac{k_p^2 a^2}{2}[0.6159 - \ln(k_p a)]. \tag{7}$$

This weak logarithmic dependence has often been neglected in subsequent works,[2–4] and this leads to an inaccuracy of a factor of 4 for $k_p a$ ranging from 10^{-4} to 10^{-1}.

The expression for $R(0)$ for Gaussian bunches with $\rho_\perp(r) = e^{-r^2/2\sigma_r^2}$ is

$$R(0) = \left(\frac{k_p^2\sigma_r^2}{2}\right)(e^{k_p^2\sigma_r^2/2})\Gamma\left(0, \frac{k_p^2\sigma_r^2}{2}\right), \tag{8}$$

where $\Gamma(\alpha,\beta) = \int_\beta^\infty t^{\alpha-1}e^{-t}dt$. In the limit $k_p\sigma_r \ll 1$, Eq. (8) can be expanded asymptotically as

$$R(0) = k_p^2\sigma_r^2[0.05797 - \ln(k_p\sigma_r)]. \tag{9}$$

Next, we closely examine and compare these expressions numerically. To make the comparison, we note that for the same number of beam particles and the same peak density, we must use $a = \sqrt{2}\sigma_r$. In Fig. 1, we plot the ratio of Eq. (6) and Eq. (8) by using this relationship between a and σ_r.

From Fig. 1(a) we see that $R(0)$ for the two profiles differ by at most 20% near $k_p\sigma_z \approx 1.35$ and are nearly identical for $k_p\sigma_z \ll 1$ or $k_p\sigma_z \gg 1$. In Fig. 1(b), for a transverse Gaussian profile, we plot both the full expression for $R(0)$ [Eq. (8)] and the asymptotic expression for small $k_p\sigma_r$ [Eq. (9)]. This shows that the asymptotic expression is extremely accurate for $k_p\sigma_r < 0.5$.

Combining Eqs. (4) and (8), we obtain an expression for the wake amplitude for a bi-Gaussian shaped drive beam:

$$E_{za} = \sqrt{2\pi}\left(\frac{mc\omega_p}{e}\right)\left\{\left(\frac{q}{e}\right)\left(\frac{n_b}{n_p}\right)(k_p\sigma_z e^{-k_p^2\sigma_z^2/2})\left(\frac{k_p^2\sigma_r^2}{2}\right) \times (e^{k_p^2\sigma_r^2/2})\Gamma\left(0, \frac{k_p^2\sigma_r^2}{2}\right)\right\}. \tag{10}$$

This can be rewritten in terms of the total particle number $N = (2\pi)^{3/2}\sigma_r^2\sigma_z n_b$:

$$E_{za} = qNk_p^2\left\{(e^{-k_p^2\sigma_z^2/2})(e^{k_p^2\sigma_r^2/2})\Gamma\left(0, \frac{k_p^2\sigma_r^2}{2}\right)\right\}. \tag{11}$$

This explicitly shows the k_p^2 dependence of the wake amplitude for a beam with fixed N, $k_p\sigma_z$, and $k_p\sigma_r$. To get the optimal wakefield amplitude for a beam with given N, σ_z, and σ_r, we rewrite this formula as

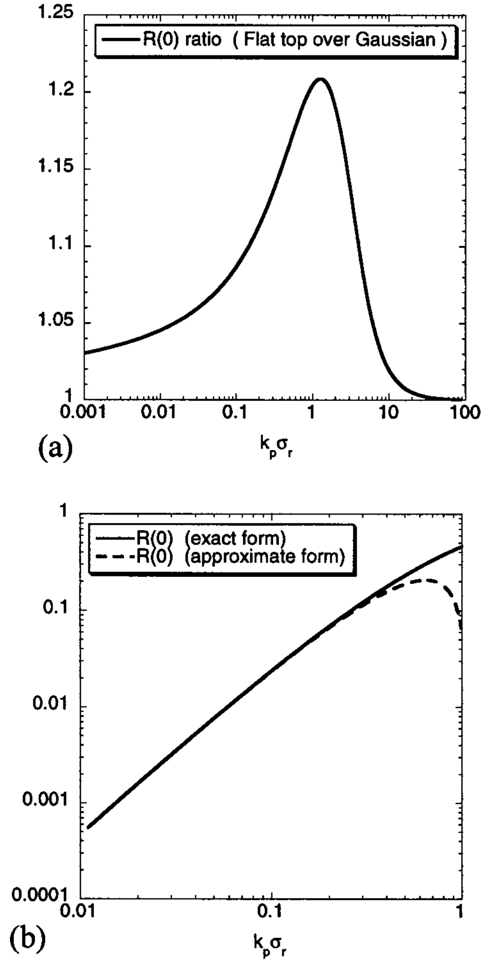

FIG. 1. (a) The $R(0)$ ratio between flat top and Gaussian profiles. (b) Comparison between exact form and asymptotic form for a Gaussian profile.

$$E_{za} = \frac{qN}{\sigma_r\sigma_z}\left\{(k_p\sigma_z)(e^{-k_p^2\sigma_z^2/2})(k_p\sigma_r)(e^{k_p^2\sigma_r^2/2})\Gamma\left(0, \frac{k_p^2\sigma_r^2}{2}\right)\right\} \equiv \frac{qN}{\sigma_r\sigma_z}\Omega(k_p\sigma_z, k_p\sigma_r), \tag{12}$$

where $\Omega(k_p\sigma_z, k_p\sigma_r)$ can also be viewed as a function of $k_p\sigma_z$ and $r_a \equiv \sigma_r/\sigma_z$, and r_a is defined as the beam's aspect ratio. Next, we maximize this expression for fixed particle number N, σ_z, and σ_r, i.e., we find the optimal plasma density. Although the optimal $k_p \equiv k_{p1}$ depends on both σ_z and σ_r, the maximum value for Ω depends only on the aspect ratio r_a. So the maximum wake amplitude can be written as

$$E_{zM} = \frac{qN}{\sigma_r\sigma_z}\Theta\left(\frac{\sigma_r}{\sigma_z}\right), \tag{13}$$

where $\Theta(\sigma_r/\sigma_z) \equiv \Omega(k_{p1}\sigma_z, k_{p1}\sigma_r)$ and $\partial\Omega/\partial k_p = 0$ for $k_p = k_{p1}$.

In Fig. 2, we plot the function $\Theta(\sigma_r/\sigma_z)$ and the function $\Omega(k_{p2}\sigma_z, k_{p2}\sigma_r)$, where $k_{p2} = \sqrt{2}/\sigma_z$. It can clearly be seen that they agree very well as long as $\sigma_r/\sigma_z < 0.1$. We also note that the ratio k_{p1}/k_{p2} is unity for r_a near zero and that it falls to zero as r_a increases. This is because we are keeping the particle number and not n_b/n_p fixed. As r_a is increased then

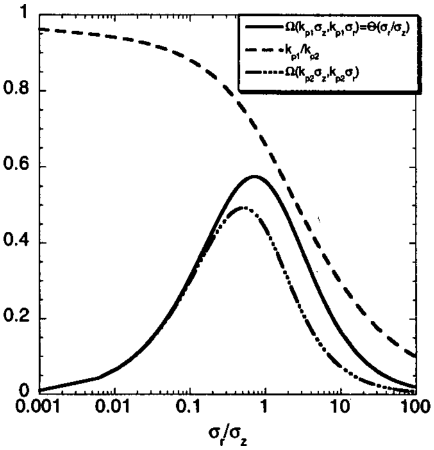

FIG. 2. $\Omega(k_{p1}\sigma_z, k_{p1}\sigma_r)$, $\Omega(k_{p2}\sigma_z, k_{p2}\sigma_r)$, and k_{p1}/k_{p2}.

n_b/n_p begins to drop and the wake amplitude becomes very small unless the bunch is shortened. If instead we kept n_b/n_p fixed, then in the wide beam limit [see Eq. (4) for $R(0)=1$], the optimal wake would once again be obtained for $k_p\sigma_z/\sqrt{2}=1$.

Bruhwiler *et al.*[9] have also investigated how the optimum density depends on the aspect ratio. They started from the formula given in Ref. 3 which attempted to merge the small $k_p\sigma_r$ and large $k_p\sigma_r$ results into a single formula. However, due to the logarithmic divergence it is not so simple to merge the two regimes. However, it is interesting to note that the formula for the optimum plasma density obtained by Bruhwiler *et al.* differs from our exact results (Fig. 2) by at most 15%.

To make connection with previous results we define a new function $\Pi(\sigma_r/\sigma_z)=\Theta(\sigma_r/\sigma_z)/(\sigma_r/\sigma_z)$ (which is plotted in Fig. 3). Using this function, we can rewrite E_{zM} as

$$E_{zM}=\frac{qN}{\sigma_z^2}\Pi\left(\frac{\sigma_r}{\sigma_z}\right). \tag{14}$$

The function $\Pi(\sigma_r/\sigma_z)$ is a relatively slowly changing logarithmic function. To obtain useful scaling laws this weak dependence was neglected leading to the well-known $1/\sigma_z^2$ scaling law cited in the literature.[4]

However, although this dependence is weak it is still significant over the range of parameters being used in present experiments[1,5,6] and being considered in future experiments. In the limit of $\sigma_r/\sigma_z \ll 1$ it is possible to obtain a very accurate asymptotic expansion for $\Pi(\sigma_r/\sigma_z)$. If we use the result from Eq. (9) in Eq. (11) and then maximize the expression with respect to k_p^2, we recover the result that the optimal normalized wake occurs for $k_p\sigma_z/\sqrt{2}=1$. This was shown in Fig. 2 where the optimal normalized field and that for $k_p\sigma_z/\sqrt{2}=1$ are identical for small r_a. Using this fact, it is straightforward to obtain the asymptotic expression

$$\Pi\left(\frac{\sigma_r}{\sigma_z}\right)\approx\frac{2}{e}\left\{-0.577-2\ln\left(\frac{\sigma_r}{\sigma_z}\right)\right\}$$
$$\approx\frac{4}{e}\{0.057\,97-\ln(k_p\sigma_r)\}. \tag{15}$$

Therefore, in the small r_a limit, we find

$$E_{zM}=\frac{qN}{\sigma_z^2}\Pi\left(\frac{\sigma_r}{\sigma_z}\right)\approx\frac{qN}{\sigma_z^2}\left\{\frac{4}{e}[0.057\,97-\ln(k_p\sigma_r)]\right\} \tag{16}$$

or in normalized units

$$\frac{eE_{zM}}{mc\omega_p}\approx 1.3\frac{q}{e}\frac{n_b}{n_p}k_p^2\sigma_r^2\ln\left(\frac{1}{k_p\sigma_r}\right), \tag{17}$$

where we have assumed that $k_p\sigma_r \ll 1$ so that the 0.057 97 constant can be neglected. We can also rewrite this in the following form for comparisons with experiments:

$$E_{zM}\approx(236\ \text{MV/m})\left(\frac{q}{e}\right)\left(\frac{N}{4\times10^{10}}\right)$$
$$\times\left(\frac{0.06\ \text{cm}}{\sigma_z}\right)^2\ln\left(\sqrt{\frac{10^{16}\ \text{cm}^{-3}}{n}}\frac{50\ \mu\text{m}}{\sigma_r}\right). \tag{18}$$

This engineering formula is identical to Eq. (1) of Refs. 2 and 3 except for the natural logarithmic term. As we have noted before, the slow logarithmic term can vary by factors of 4 for typical experimental parameters, so when making comparisons to experiments one needs to include this term.

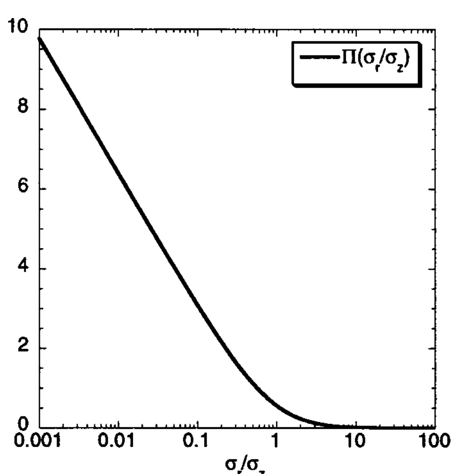

FIG. 3. A plot of the $\Pi(\sigma_r/\sigma_z)=\Theta(\sigma_r/\sigma_z)/(\sigma_r/\sigma_z)$.

III. BREAKDOWN OF LINEAR-FLUID THEORY

The above calculations are strictly speaking only valid in the linear-fluid limit. Linear theory is valid when the perturbed density is less than the background density, $n_1/n_p \ll 1$, when the fluid velocity is less than $v_\phi \cong c$, $\nu/c \ll 1$, and when the normalized electric field is less than unity, $eE_{zM}/mc\omega_p \equiv \varepsilon \ll 1$. In order that $n_1/n_p \ll 1$, the peak beam density n_b must also be less than the background density, $n_b/n_p \ll 1$.

Cold-fluid theory is valid when individual particle trajectories do not cross. For wide beams, i.e., the 1D limit, all of the above conditions are equivalent and simultaneously satisfied. However, for narrow bunches the story is not clear. For a beam with any fixed amount of charge or charge per unit length, one can shrink the spot size down to a size for

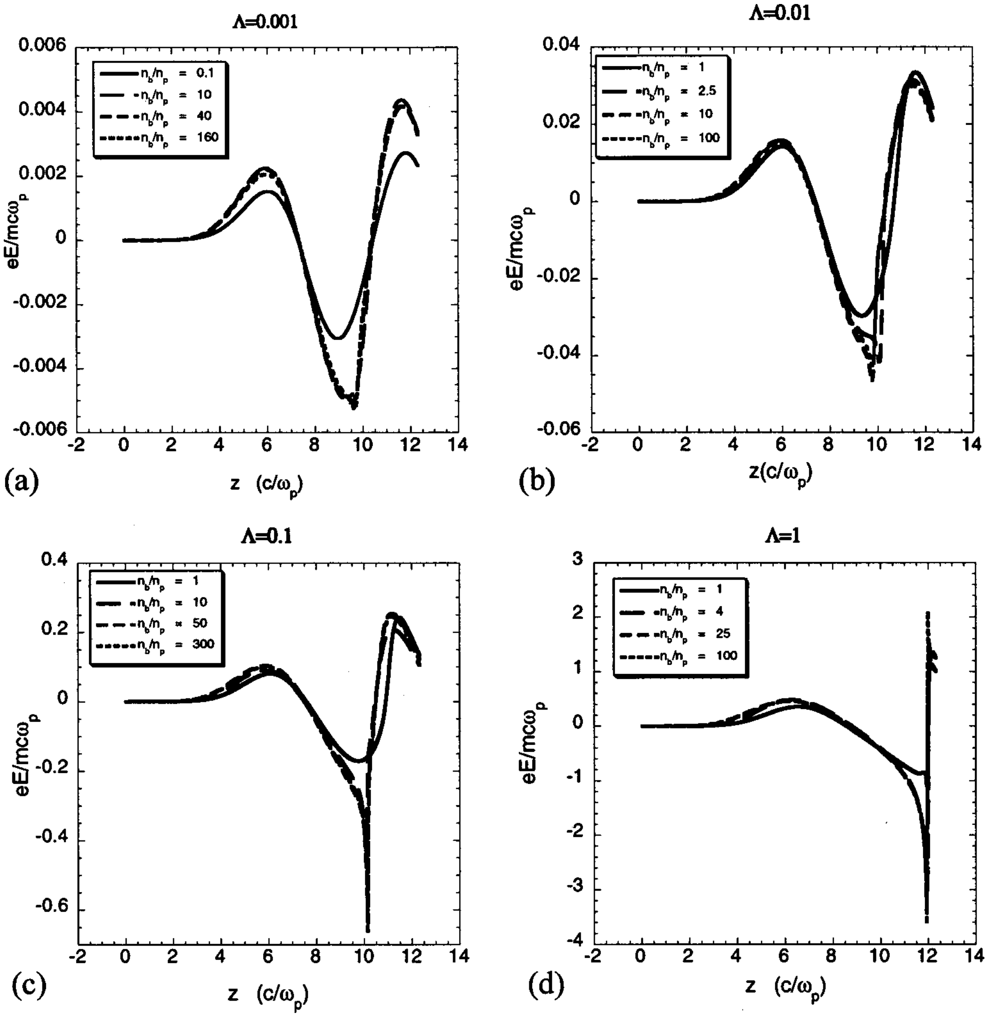

FIG. 4. Saturation of wakefield for electron driver: in each figure, we decrease $k_p\sigma_r$ (at the same time increase n_b/n_p) by keeping Λ fixed. We see the wake forms will saturate roughly when n_b/n_p is larger than 10, and (a) $\Lambda=0.001$, (b) $\Lambda=0.01$, (c) $\Lambda=0.1$, and (d) $\Lambda=1$ (the $z=0$ point is $6c/\omega_p$ ahead of the beam center).

which $n_b/n_p>1$, but for which the normalized electric field can still be less than unity. This is possible since as seen in Eq. (17) the dominant term for the latter is proportional not to n_b/n_p but rather to $(n_b/n_p)k_p^2\sigma_r^2$. However, the spot size can always be reduced further such that the normalized electric field gets large because of the logarithmic divergence in Eq. (17). Such a divergence is obviously unphysical. The resolution is that fluid theory breaks down for very narrow bunches because the plasma electrons are predominantly expelled radially outward, and if $n_b/n_p>1$ the trajectories of electrons that originate within the beam cross each other. Interestingly, linear theory of arbitrary shaped bunches is based on a Green's function which is not a valid solution to linear theory. The point is that what matters is not whether the solution for the wake due to a δ function is valid but rather whether the wake obtained by integrating the Green's function over the beam distribution is linear.

In the linear-fluid regime, the plasma response to electron or positron beams is similar except for a change of charge sign. However, when n_b increases, the wake structure and amplitude will change due to the breakdown of fluid theory and the appearance of nonlinear effects. The plasma has a very different nonlinear response to electron or positron beams (an electron beam will blow plasma electrons away, while a positron beam will suck them in). The breakdown of fluid theory inevitably occurs for positron generated wakes because trajectory crossing occurs as electrons reach the axis after they are sucked in.

It has been argued that the linear-fluid limit is still a surprisingly useful guide for predicting wake amplitudes even in the nonlinear and/or blowout regime. To investigate this, we compare the linear-fluid theory expressions given above against fully nonlinear electromagnetic PIC simulations (both fully explicit and quasistatic). We use the codes OSIRIS (Ref. 10) and QuickPIC.[11] These two codes give identical results for wakes excited by ultrarelativistic charged particle beams.

To quantify the usefulness of linear-fluid theory, we begin examining through PIC simulations what happens as we decrease $k_p\sigma_r$ while keeping $k_p\sigma_z$ and N (i.e., Λ) fixed. In Fig. 4 we plot the dependence of the normalized wake amplitude on $k_p\sigma_r$ for four different beam charges $\Lambda=0.001$, 0.01, 0.1, and 1. For each value of Λ we plot line outs along the axis of the electric field in units of $mc\omega_p/e$ for four different values of $k_p\sigma_r$ or equivalently four values of n_b/n_p. The figures show that for each value of Λ the field amplitude increases as n_b/n_p is increased until n_b/n_0 exceeds ~ 10. After n_b/n_p increases beyond ~ 10 neither the amplitude nor the wave form shape changes. Based on these results we can define a critical value for $k_p\sigma_r$ which roughly corresponds to a beam density $n_b/n_p \approx 10$, i.e., $k_p\sigma_r \approx \sqrt{\Lambda/10}$.

This kind of behavior can be qualitatively understood as follows: If the blowout radius r_{bm} is much larger than the beam radius σ_r, then any further reduction in the beam radius can only cause a small change to the plasma response to the beam. Therefore, the wakefield changes very little after $\sigma_r \ll r_{bm}$. A rough estimate of r_{bm} is $k_p r_{bm} \approx 2\sqrt{\Lambda}$, where $\sqrt{\Lambda}$ is the charge neutralizing radius. In addition, since $k_p\sigma_r = \sqrt{\Lambda/(n_b/n_p)}$, the ratio of $r_{bm}/\sigma_r \approx 2\sqrt{n_b/n_p}$; for example, $r_{bm}/\sigma_r \geqslant 10$ requires that $n_b/n_p \geqslant 25$. This explains why the wake does not change much when $k_p\sigma_r$ is very small. We will provide a more quantitative explanation in a future publication.

Another thing worth noting from Fig. 4 is how the wave form of the wake depends on Λ. For very small charge ($\Lambda = 0.001$), the wakes basically have sinusoidal wave forms for all spot sizes. However, for large Λ (0.1 and 1), the wakes become elongated and have very sharp spikes. The elongation is due to nonlinear frequency shifts due to relativistic mass effects, because for large Λ the plasma electrons acquire relativistic velocities. The formation of the spike occurs when we have large Λ and small spot sizes, $k_p\sigma_z < 1$, which is called the blowout regime.

The wakes produced by positron beams depend on Λ and spot size in a more complicated manner than for electron wakes. This is shown in Fig. 5 where we plot line outs of the electric field along the axis for positron drivers. As in Fig. 4, for each plot we keep Λ fixed and vary $k_p\sigma_r$. The first thing worth noting is that the positron wake structure can change dramatically by decreasing $k_p\sigma_r$. For relatively large charge (i.e., $\Lambda = 0.1, 1$), multipeak structures show up in the decelerating fields as $k_p\sigma_r$ is decreased. This can be roughly explained by the phase mixing of plasma electrons: plasma electrons at different initial positions reach the axis at different times. For example, plasma electrons far away from the beam typically oscillate about the axis with a frequency very close to ω_p, but plasma electrons very close to the beam center can have a frequency close to $\omega_b = \sqrt{n_b/n_p}\omega_p$, which can be many times larger than ω_p for very narrow beams. Therefore, these electrons arrive at the axis at different times. This leads to spaced density peaks of the frequency between ω_p and ω_b.

This can also explain why the accelerating peaks do not have multipeak structures. The accelerating fields are behind the beam, and in this region the plasma electrons will all roughly oscillate at the same frequency ω_p. Although positron wakes have more complicated structures than electron wakes, they still saturate as the spot size is reduced. The difference is that the critical $k_p\sigma_r$ for positron wakes is around $\sqrt{\Lambda}$ which corresponds to $n_b/n_p = 1$ rather than 10 as was the case for electron drivers.

The above discussion shows that the linear-fluid expression cannot be used when $n_b/n_p \gtrsim 10$ for electron drivers and when $n_b/n_p \gtrsim 1$ for positron drivers. Physically this occurs due to the extreme trajectory crossing that occurs in the nonlinear wakefield regime. It also shows that if we have calculated the wake amplitude for $n_b/n_p = 10$ for all spot sizes $k_p\sigma_r$, we can give accurate estimates for the wake for any

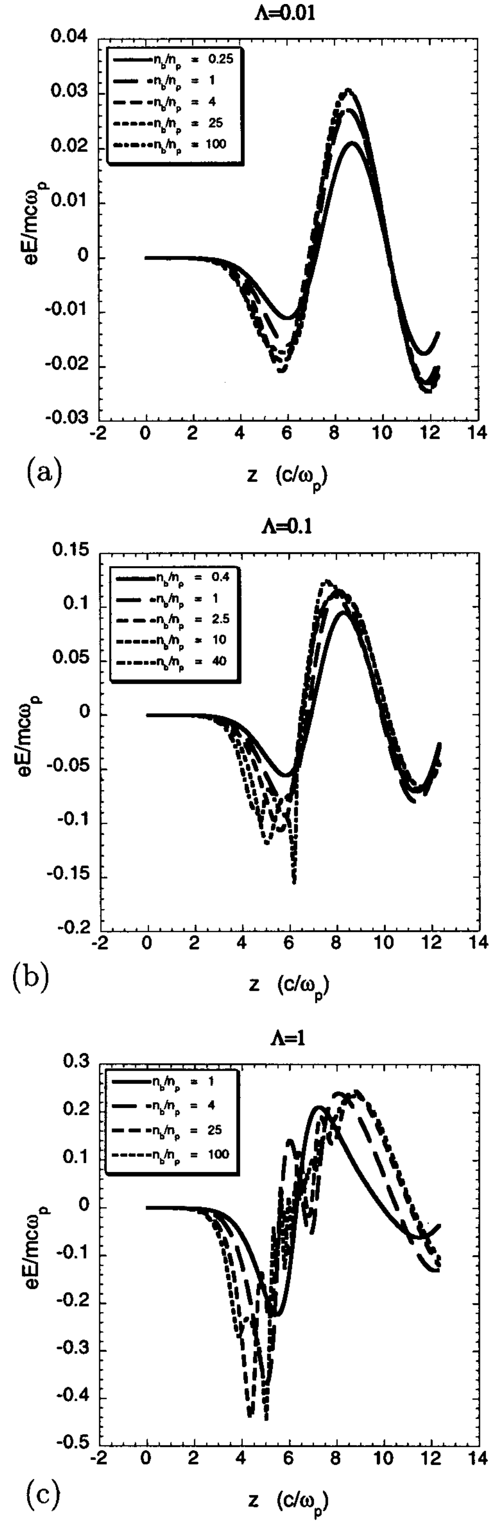

FIG. 5. Saturation of wakefield for positron driver: in each figure, we decrease $k_p\sigma_r$ while simultaneously increasing n_b/n_p and keeping Λ fixed. We see the wake forms will saturate roughly when n_b/n_p is larger than 1, and (a) $\Lambda = 0.01$, (b) $\Lambda = 0.1$, and (c) $\Lambda = 1$ (the $z = 0$ point is $6c/\omega_p$ ahead of the beam center).

value of $n_b/n_p \gtrsim 10$. This is done by finding the case where $n_b/n_p = 10$ for a larger spot size but with the same charge per unit length Λ.

The above discussion has not addressed to what extent linear-fluid theory works when $n_b/n_p \leqslant 10$. To address this,

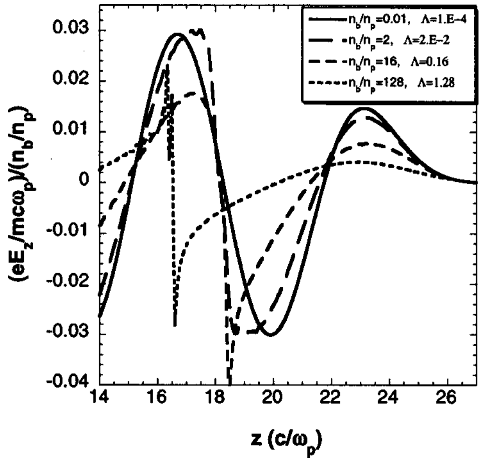

FIG. 6. Wake structure for electron drivers: we plot the ratio of normalized electric field over n_b/n_p, as a function of distance behind the wake, for $k_p\sigma_z=\sqrt{2}$ and $k_p\sigma_r=0.1$ (the beam center is at $z=23c/\omega_p$).

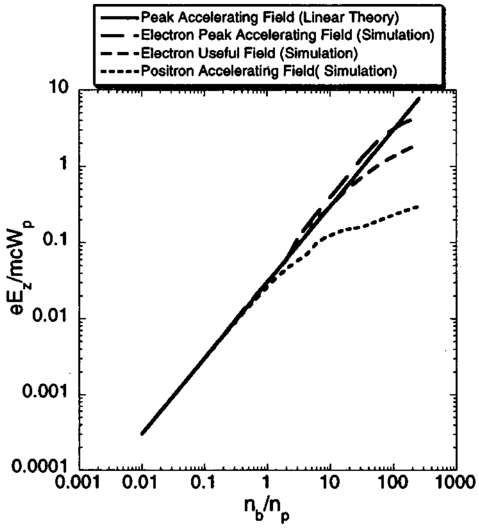

FIG. 8. Peak accelerating field compared with linear theory.

we have carried out a series of simulations for a given plasma density n_p and fixed beam shapes (Gaussian beams with fixed σ_r and σ_z). We vary beam density n_b from a value much smaller than n_p to a value much larger than n_p by changing N. As N is increased, the wake structure and amplitude will evolve from a regime where linear theory is valid into a nonlinear regime. For one set of runs we used $k_p\sigma_z=\sqrt{2}$, $k_p\sigma_r=0.1$ and the results are shown in Figs. 6 and 7 for electron and positron drivers, respectively. These results illustrate the transition of the wake structure (the peak accelerating field, the wake wavelength, and the transformer ratio) for both electron and positron beams as the beam particle number is increased.

Several points are worth noting. We plot the ratio of electric field over n_b/n_p, because in linear theory the field is proportional to n_b/n_p, when $k_p\sigma_z$ and $k_p\sigma_r$ are fixed, and the wake structure does not change. This choice helps Figs. 6 and 7 to illustrate how the wake structure in the simulations differ from the predictions of linear theory. In Fig. 6, it can be seen that as n_b/n_p is increased, the peak accelerating field remains relatively constant while the decelerating field decreases. Therefore, the transformer ratio gradually increases. At the highest value of n_b/n_p the wavelength elongates and this is due to the fact that for such a high beam charge the plasma particles acquire relativistic energies. Despite this gross change to the wavelength, the peak field is still close to the linear prediction. Therefore, significant deviation from linear theory for the peak accelerating field does not occur until the normalized electric field $(eE/mc\omega_p)$ approaches unity. This is also true in the 1D regime. On the other hand, in Fig. 7 it can be seen for positron drivers that the accelerating as well as the decelerating field change dramatically as n_b/n_p increases beyond 2. Therefore, for narrow positron bunches the relevant nonlinear parameter is n_b/n_p and not Λ.

To make the transition between linear-fluid theory and nonlinear wake dynamics (either blowout or suck-in) clearer, we plot in Figs. 8 and 9 the peak accelerating fields and the peak decelerating fields against those predicted by linear theory from a series of 30 simulations.

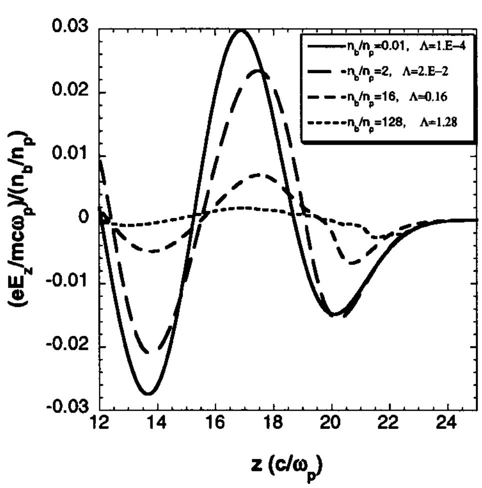

FIG. 7. Wake structure for positron drivers: we plot the ratio of normalized electric field over n_b/n_p, as a function of distance behind the wake, for $k_p\sigma_z=\sqrt{2}$ and $k_p\sigma_r=0.1$ (the beam center is at $z=20c/\omega_p$).

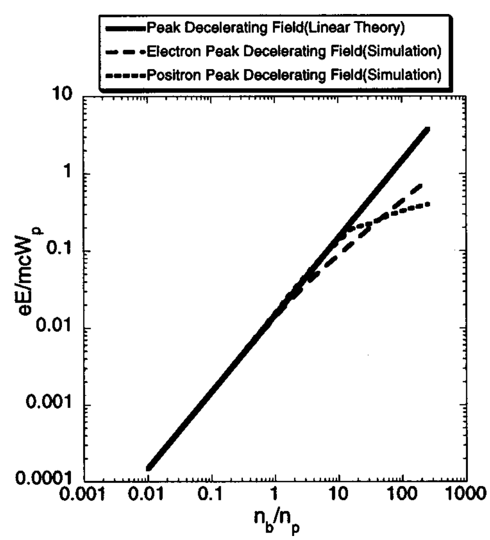

FIG. 9. Peak decelerating field compared with linear theory.

In these runs we set $k_p\sigma_z=\sqrt{2}$, $k_p\sigma_r=0.1$ while n_b/n_p was varied by varying N. We plot the fields in units of $mc\omega_p/e$. For the electron driver runs, we plot the peak accelerating and decelerating fields as well as the "useful" accelerating field. We adopt a similar definition for the useful field as given in Ref. 12. As shown in Fig. 6, for nonlinear wakes, the structure of the accelerating field contains a part with a linear slope and a deep spike. If the linear slope section was continued then the useful is defined where it intersects the actual curve. For sinusoidal fields we define the peak and useful fields to be the same. As seen in Fig. 6, the peak and useful fields are equal (indicating that the field had a "sinusoidal" structure) for n_b/n_p as high as 10. For higher n_b/n_p the useful field is lower than linear theory while the peak field is still approximately given by linear theory until n_b/n_p exceeds 100 (or Λ exceeds unity). The decelerating field deviates from linear theory as soon as n_b/n_p exceeds 10. On the other hand, for positron drivers the accelerating field deviates from linear theory when n_b/n_p exceeds unity and the decelerating field agrees with linear theory until n_b/n_p exceeds 10.

IV. SUMMARY

In this paper, we have revisited linear-fluid wakefield theory. We have obtained expressions for the wakes of bi-Gaussian electron and positron drivers for arbitrary spot sizes. We showed that these expressions give very similar results to those from radial flat top profiles. We obtained the proper expression for the wake amplitude from narrow bunches, $k_p\sigma_r \ll 1$, which we rewrite here for convenience [Eq. (18)],

$$E_{zM} \approx (236\ \mathrm{MV/m})\left(\frac{q}{e}\right)\left(\frac{N}{4\times 10^{10}}\right) \times \left(\frac{0.06\ \mathrm{cm}}{\sigma_z}\right)^2 \ln\left(\sqrt{\frac{10^{16}\ \mathrm{cm}^{-3}}{n}}\frac{50\ \mu\mathrm{m}}{\sigma_r}\right).$$

We then used fully nonlinear PIC simulations to examine the validity and usefulness of linear-fluid theory as the normalized charge per unit length, $\Lambda \equiv n_b/n_p k_p^2\sigma_r^2$, is increased. We found that as the spot size is decreased, fluid theory eventually breaks down causing the logarithmic divergence to saturate. Physically, the saturation occurs because if the blowout radius greatly exceeds the beam spot size, then reducing the spot size has little effect. In the multidimensional nonlinear wakefield regime where electrons move radially inward or outward there is multiple trajectory crossing and fluid theory breaks down.

Based on numerous simulations, including many with parameters different than those in Figs. 6–9, we can make the following generalization for the narrow beam limit $(k_p\sigma_r<0.3, k_p\sigma_z\sim\sqrt{2})$ and the weakly nonlinear limit, $\Lambda<1$.

For electron drivers, the useful accelerating fields agree with linear theory up to $n_b/n_p\approx 10$, and then becomes smaller than linear theory, while the decelerating field agrees with linear theory only up to $n_b/n_p\approx 1$.

For positron drivers, both the peak accelerating fields and the peak decelerating fields agree with linear theory up to $n_b/n_p\approx 1$.

Combining the results of linear theory and the discussion above, we can give approximate expressions for plasma wakefield amplitudes in the narrow beam limit for Λ smaller than 1.

For an electron driver, if $n_b/n_p\leqslant 10$, we just use the linear expression in Eq. (17) which is rewritten here for convenience,

$$\frac{eE_{zM}}{mc\omega_p} \approx 1.3\frac{q}{e}\frac{n_b}{n_p}k_p^2\sigma_r^2 \ln\left(\frac{1}{k_p\sigma_r}\right)$$

and for $n_b/n_p>10$, instead use the following expression:

$$\frac{eE_{zM}}{mc\omega_p} \approx 1.3\frac{q}{e}\frac{n_b}{n_p}k_p^2\sigma_r^2 \ln\left(\frac{1}{\sqrt{\Lambda/10}}\right). \tag{19}$$

For a positron driver, if $n_b/n_p\leqslant 1$, just use the linear expression [Eq. (17)]

$$\frac{eE_{zM}}{mc\omega_p} \approx 1.3\frac{q}{e}\frac{n_b}{n_p}k_p^2\sigma_r^2 \ln\left(\frac{1}{k_p\sigma_r}\right)$$

and for $n_b/n_p>1$, instead use the following expression:

$$\frac{eE_{zM}}{mc\omega_p} \approx 1.3\frac{q}{e}\frac{n_b}{n_p}k_p^2\sigma_r^2 \ln\left(\frac{1}{\sqrt{\Lambda}}\right). \tag{20}$$

In the highly nonlinear regime, $\Lambda\gg 1$, where relativistic effects are dominant (the wavelength increases due to the electron mass change and the full electromagnetic character of the fields in the wake are important), the above expressions can no longer be used. In this regime, simulations show that the wake amplitude is much smaller than that given by the above expressions.

ACKNOWLEDGMENTS

The authors acknowledge useful conversations with members of the E-164 collaboration.

This work was supported by U.S. Department of Energy under Grant Nos. DE-FE02-01ER41179, DE-FE03-92–ER40727, DE-FG03-03NA00065, and DE-FG02-03ER54721. The simulations were performed on the IBM SP @NERSC.

[1] M. J. Hogan, R. Assmann, F.-J. Decker*et al.*, Phys. Plasmas **7**, 2241 (2000).
[2] S. Lee, T. Katsouleas, R. Hemker, and W. B. Mori, Phys. Rev. E **61**, 7014 (2000).
[3] S. Lee, T. Katsouleas, R. Hemker, E. S. Dodd, and W. B. Mori, Phys. Rev. E **64**, 045501(R) (2001).
[4] S. Lee, T. Katsouleas, P. Muggli *et al.*, Phys. Rev. ST Accel. Beams **5**, 011001 (2002).
[5] B. E. Blue, C. E. Clayton, C. L. O'Connell *et al.*, Phys. Rev. Lett. **90**, 214801 (2003).
[6] P. Muggli, B. E. Blue, C. E. Clayton *et al.*, Phys. Rev. Lett. **93**, 014802 (2004).

[7] P. Chen, J. M. Dawson, R. W. Hu, and T. Katsouleas, Phys. Rev. Lett. **54**, 693 (1985).
[8] T. Katsouleas, S. Wilks, P. Chen, J. M. Dawson, and J. J. Su, Part. Accel. **22**, 81 (1987).
[9] D. Bruhwiler, D. A. Dimitrov, J. R. Cary, E. Esarey, and W. P. Leemans, *Proceedings of Particle Accelerator Conference*, edited by J. Chew, P. Lucus, and S. Webber (IEEE, Piscataway, NJ, 2003), p. 734, IEEE Cat. No. 03CH37423.
[10] R. Hemker, Ph.D thesis, University of California, Los Angeles, 2000.
[11] C. Huang, Master thesis, University of California, Los Angeles, 2003.